External control of dissipation in a nanometer-scale radiofrequency mechanical resonator

A.N. Cleland *, M.L. Roukes

Condensed Matter Physics 114-36, California Institute of Technology, Pasadena, CA 91125, USA

Abstract

We demonstrate a technique by which the quality factor of a magnetically-actuated mechanical resonator is controlled by an external electrical circuit. Modulation of this parameter is achieved by local variation of the electrical impedance presented to the resonator at its resonance frequency. We describe a theory that explains this result as arising from eddy currents in the external electrical circuit, which are driven by electromotive forces generated through motion of the resonator in the applied magnetic field. The theory is in good agreement with the induced variation in quality factor that we observe. © 1999 Elsevier Science S.A. All rights reserved.

Keywords: Dissipation; Nanometer; Micromachining; Radiofrequency; Resonator

1. Introduction

There has recently been considerable interest in micro- and nano-machined mechanical resonators, both from the point of view of fundamental physics [1–4] and for applications as sensors and modulators [5–13]. Mechanical resonators made from single crystal materials such as Si can be fabricated so that the mechanical losses are dominated by defects or phonon emission in the resonator structure [1], and nanometer-scale resonators might provide a tool for investigating these processes at high frequencies. Important technological applications of mechanical resonators include frequency-agile high speed signal processing, radiofrequency filter design [14,15], scanned probe microscopy, and charge detection [16]; for these, external control of the resonance frequency and resonance width (quality factor) would be of great utility.

A primary consideration for either the characterization or application of these devices is the degree to which these resonators are coupled to, and affected by, the outside world. Inducing or detecting motion in micromechanical structures is often done using electronic means, achieved by magnetic [2,3,7,13], electrostatic [1,5,6,8] or piezoresistive [9] coupling. The possibility exists that the external electrical circuit itself may affect the resonator performance, causing an apparent change of the mechanical parameters. This offers the interesting potential for external control, but also makes measurement of the intrinsic mechanical properties more difficult. In this paper we describe a technique whereby the external electrical damping can be measured and controlled locally, enabling us to manipulate the resonance width and slightly modulate the resonance frequency.

2. Experimental

The resonator we used for this experiment has a fundamental resonance frequency of 3.869 MHz, and was fabricated from a silicon-on-insulator (SIMOX) substrate with a Si layer thickness of 200 nm and an oxide thickness of 400 nm. First, two planar conducting leads terminating in wire bond pads were patterned using electron beam (e-beam) lithography

---

* Corresponding author. Department of Physics, University of California at Santa Barbara, Santa Barbara, CA 93106, USA
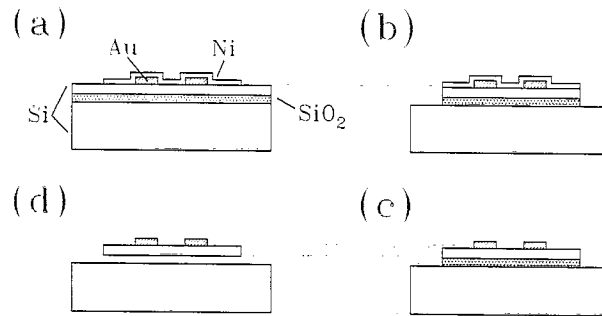
Fig. 1. Cross-sectional views of processing steps. (a) SIMOX substrate with patterned Au leads and Ni mask. (b) Following anisotropic RIE etch of Si and SiO$_2$ layers. (c) Following removal of Ni mask. (d) Following sacrificial etch of SiO$_2$ layer.

followed by evaporation and liftoff of 5 nm of Cr and 35 nm of Au; we used Au for its ability to withstand the concentrated acid used later in the processing. Second, the mechanical structure was defined by a second layer of e-beam lithography and liftoff of 100 nm of Ni, which forms an extremely durable mask for the subsequent, fluorine-based, anisotropic reactive ion etching (RIE) of the substrate [13]. Finally, the Ni was removed using a wet chemical etch, and the active region of the structure suspended by etching the underlying oxide layer using concentrated hydrofluoric acid. The sample was rinsed in ethanol and dried in a CO$_2$-based critical point dryer to avoid stiction problems caused by surface tension. The steps involved in the processing are shown in Fig. 1. Electrical contacts were made by connecting 25 μm diameter Au wires from the Au wire bond pads to a chip carrier. A SEM micrograph of the device is shown in Fig. 2. Separate drive and sense leads were used to reduce direct coupling of the drive signal into the detection amplifier, thus increasing detection sensitivity. The structure is actually designed as a double resonator, with a distinct, smaller beam suspended from the larger flexural plate; however, all measurements were performed at the fundamental resonance of the larger plate, where the motion of the smaller beam very accurately follows that of the plate. Rectangular cutouts at the ends of the plate reduce its effective spring constant, making it more flexible and giving a lower resonance frequency.
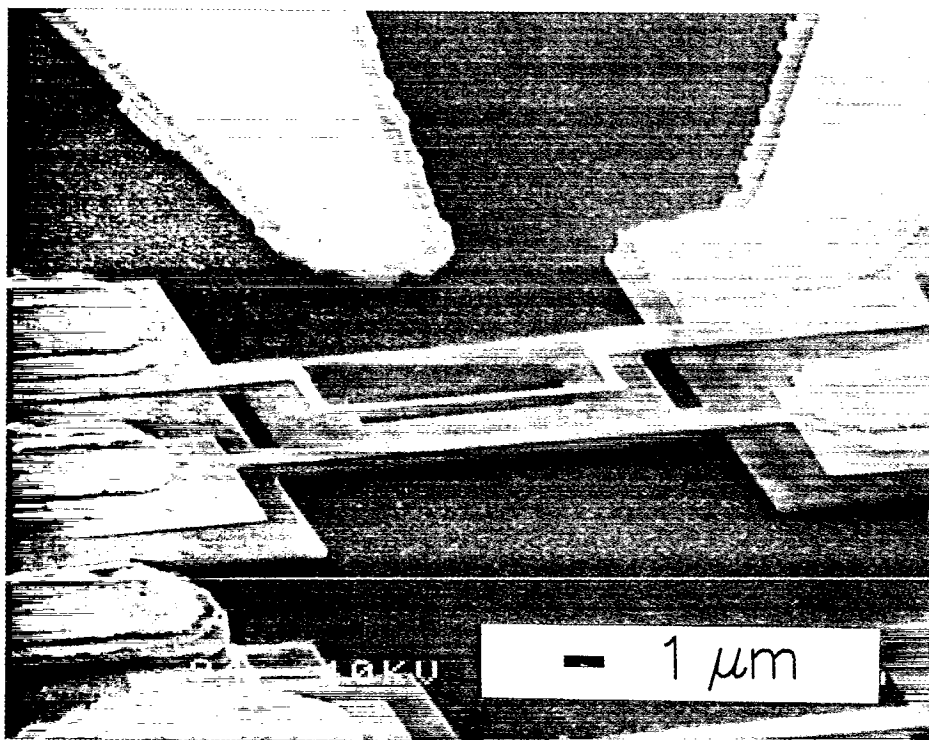

Fig. 2. SEM micrograph of the resonator, showing the suspended Si mechanical structure with separately defined metallic leads for drive and detection of the resonance. The drive lead runs along one side of the suspended structure, while the sense lead runs along the central area of the resonator. The larger plate is 15 μm long by 6 μm wide.

3. Discussion

A doubly-clamped flexural beam, with length l, width w and thickness d in the direction of motion, has a fundamental resonance frequency $f_0 = \omega_0/2\pi = 1.03(E/\rho)^{1/2}d/l^2$ where E is Young's modulus and ρ the density (for Si, $E_{\langle 100 \rangle} = 1.69 \times 10^{11}$ N/m^2, $\rho = 2330$ kg/m^3). For small motional amplitudes, the resonator may be treated [4] as a simple harmonic oscillator with effective mass $m = \rho dwl$ and spring constant $k = 41.7Ewd^3/l^3$. We generate a driving force on the resonator by placing it in a uniform magnetic field B parallel to the resonator plane, and passing a current $I_D(t)$ though a lead on the resonator, perpendicular to the field. A Lorentz force $F_D(t) = lBI_D(t)$ is thereby developed. The resulting displacement $y(t)$ of the midpoint of the resonator satisfies

$$m\frac{d^2 y}{dt^2}(t) + \gamma m\frac{dy}{dt}(t) + ky(t) = lBI_D(t), \tag{1}$$

where γ is the phenomenological damping coefficient. The motion of the resonator through the magnetic field generates an electromotive force (EMF) along the leads on the resonator, $V_{EMF}(t) = \xi lBdy(t)/dt$, where ξ is a constant of order unity, depending on the mode shape. For a simple beam in its fundamental flexural mode, $\xi = 0.83086$. In the absence of an external electrical circuit, or, equivalently, one with an infinite source impedance, the voltage in the frequency domain is given by

$$V_{EMF}(\omega) = \frac{j\omega\xi l^2 B^2/m}{\omega_0^2 - \omega^2 + j\omega\omega_0/Q_0}I_D(\omega), \tag{2}$$

where the unloaded quality factor $Q_0 = \omega_0/\gamma$.

The magnetically-coupled resonator is electrically equivalent to the parallel combination of a resistor R_m, an inductor L_m and a capacitor C_m, as shown in Fig. 2. The voltage across this circuit as a function of the applied current $I(\omega)$, for an infinite source impedance $Z_{ext} \to \infty$, is given by

$$V(\omega) = \frac{j\omega/C_m}{\omega_{LC}^2 - \omega^2 + j\omega/R_m C_m}I(\omega), \tag{3}$$

where $\omega_{LC} = 1/\sqrt{L_m C_m}$. Eqs. (2) and (3) clearly have the same form, and we can formally identify the model circuit parameters in terms of the mechanical properties of the resonator:

$$\begin{cases} C_m = \dfrac{m}{\xi l^2 B^2} \\[2mm] L_m = \dfrac{\xi l^2 B^2}{\omega_0^2 m} \\[2mm] R_m = \dfrac{\xi l^2 B^2}{\omega_0 m}Q_0 \end{cases} \tag{4}$$

These relations imply equality of the resonance frequencies, $\omega_{LC} = \omega_0$.

We will now explore the effect of a *finite* embedding impedance $Z_{ext}(\omega)$ on the measured properties of such a resonator. For the purposes of this discussion, we assume the external impedance $Z_{ext}(\omega)$ changes slowly over the resonance width, which is assumed to be narrow, with $Q \gg 1$. The external impedance can then be replaced by its value on resonance, $Z_{ext}(\omega) \cong R_{ext} + jX_{ext}$ with $R_{ext} = \text{Re}[Z_{ext}(\omega_0)]$ and $X_{ext} = \text{Im}[Z_{ext}(\omega_0)]$. The voltage developed across the complete circuit is then given by

$$\begin{aligned} V_L(\omega) &= \left[\frac{\omega_0^2 - \omega^2 + j\omega\omega_0/Q_0}{j\omega/C_m} + \frac{1}{R_{ext} + jX_{ext}} \right]^{-1} I(\omega) \\[2mm] &= \frac{j\omega/C_m}{\left(\omega_0^2 + \omega\omega_0 Z_c X_{ext}/|Z_{ext}|^2 \right) - \omega^2 + j\omega\omega_0\left(1/Q_0 + Z_c R_{ext}/|Z_{ext}|^2 \right)} I(\omega) \end{aligned} \tag{5}$$

using the characteristic impedance $Z_c = \sqrt{L_m/C_m}$. From this relation it is clear that the embedding impedance Z_{ext} shifts the resonance frequency and changes the resonance width. To first order in Z_c/Z_{ext}, the loaded values are given by

$$f_L = f_0\sqrt{1 + Z_c X_{ext}/|Z_{ext}|^2} \tag{6}$$

and

$$\frac{1}{Q_L} = \frac{1}{Q} + Z_c R_{ext}/|Z_{ext}|^2.$$ (7)

4. Results

In order to test this theory, and measure the effect of the external circuit on the resonator of Fig. 1, we used the circuit shown in Fig. 3, which includes two cryogenic MESFETs placed about 2 cm from the resonator. The FET labeled Q_1 is configured as a voltage-variable resistor: The drain-source conductance can be varied externally by modulating the dc gate bias V_{g1}. The parallel combination of Q_1 and the resistor R_1 presents a variable impedance to the capacitively-coupled resonator drive lead, which can be varied from about 30 Ω to 100 kΩ. A small dc bias current is applied to the FET to maintain it in the linear resistance regime. The radiofrequency signal V_{rf} supplies an alternating current, which drives the resonator.

In a separate experiment, we measured the radiofrequency reflection from the drain of Q_1 as a function of its drain-source resistance. These measurements showed that for frequencies from about 1 MHz to above 50 MHz, the reflection coefficient was in agreement with the measured dc value of the variable resistance, for values up to about 10 kΩ. This confirms that the FET configured as Q_1 presents a real impedance over the frequencies involved in this experiment.

The resonator motion was detected by coupling the sense lead on the resonator to the gate of the FET Q_2, which was dc biased by V_{g2}. The impedance presented to the resonator's sense lead is thus about 50 kΩ, including the parallel drain-gate capacitance C_{dg}. The resonator and measurement circuit were placed in vacuum in contact with a cold plate at 4.2 K in an 8 T magnetic field. These measurements could in principle have been performed at room temperature, if an air-bore magnet with sufficient field had been available; the results are not necessarily restricted to cryogenic applications. The amplitude of the drive signal V_{rf} was always small enough that the resonance shape was very accurately Lorentzian, thus avoiding the regime of anharmonic response observed with large amplitude signals, which is characteristic of these resonators. Inset to Figs. 4 and 5 we show a typical resonance curve $A(f)$ with a fit to the expected Lorentzian shape.

Measurements were then made as the resistor Q_1 was varied from 90 Ω to 8.3 kΩ, and a fit was made to extract the resonance frequency and quality factor at each resistance value. In Fig. 4 we show the measured Q_L and f_L as a function of the dc value of the variable resistor. The quality factor is seen to increase by about a factor of two as the resistance is varied over its full range, while the resonance frequency changes by about 100 parts per million.

We now apply the predictions of Eqs. (6) and (7) to these results. Inset to Fig. 3 we show a model for the high frequency circuit connected to the resonator drive lead, consisting of the metallic lead resistance $r = 30$ Ω, the coupling capacitor $C_1 = 1$ nF, and the parallel combination of the resistor R_1 and Q_1's drain-source resistance R_{ds}. Using this model, we can calculate the resonator's embedding impedance $Z_{ext}(\omega)$. Note that for the measurement described here, the electrical loading due to the sense lead is assumed negligible.

The predictions from Eqs. (6) and (7) are shown in Fig. 4 as the dotted and solid lines respectively, where the high-impedance (unloaded) limit $Q_0 = 9200$ has been fit to the data, and the unloaded resonance frequency fit to $f_0 = 3.8693$ MHz. The motion of the plate due to the driving force applied by the rf current is not precisely described by the relations for a simple clamped beam; as a result the value of ξ, and the relations of Eq. (4), are not sufficiently accurate for this system. We therefore used a finite-element numerical simulation to generate the detailed mode shape for our structure. This calculation indicates that the characteristic impedance Z_c in Eqs. (6) and (7) should be equal to 12 mΩ. Quite good agreement is found between the calculation and the measurement of the quality factor. The shift in resonance frequency,
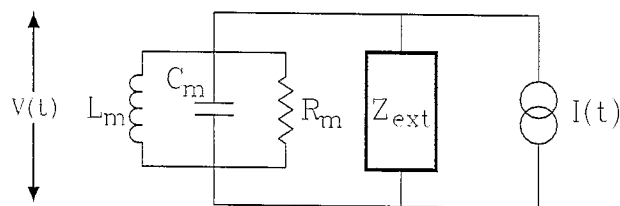

Fig. 3. High frequency circuit model, showing the RLC representation of the mechanical resonator, and a generalized impedance $Z_{ext}(\omega)$ for the external electrical environment.
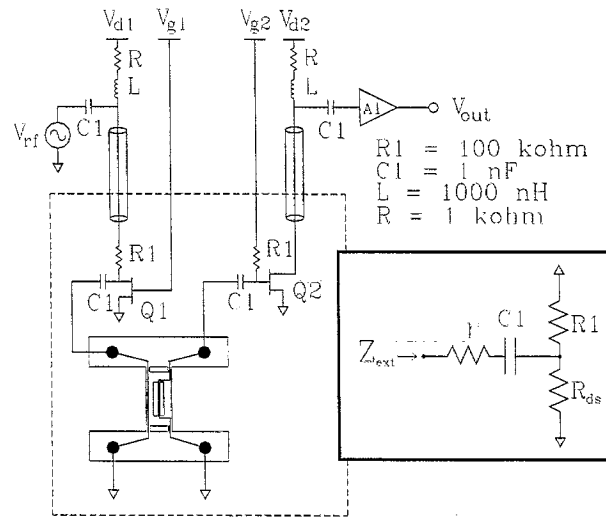
Fig. 4. System used to measure the resonator properties. The dotted outline indicates the cryogenic portion of the circuit. Amplifier A1 has a gain of 30 dB, and V_{rf} and V_{out} are the drive and detection signals for a network analyzer. Inset: simplified model for the external circuit impedance $Z_{ext}(\omega)$, showing the lead resistance r, coupling capacitance C_1, and parallel combination of resistor R_1 and drain-source resistance R_{ds}.

while of the correct sign and order of magnitude, is less well predicted; note that this shift is extremely small (about 1 part in 10^4), compared to the factor of two modulation in Q. The additional shift observed in the resonance frequency could be due to some other change in the loading impedance, such as a bias-dependent capacitance, or, alternatively, could arise through a temperature change in the resonator due to power dissipation in the FET Q_1, which at the larger values of R_{ds} will dissipate more power than at the lowest values.

The observed drop in the quality factor of the resonator at smaller values of R_{ds} is significant for applications of resonators which require narrow linewidths. For a circuit with a cable impedance of 50 Ω, a radiofrequency resonator's Q could be degraded by these coupling losses. Use of positive feedback circuitry to drive the resonator can be used to eliminate this effect [17], but for free-running oscillators, or experiments which attempt to measure intrinsic quality factors, great care must be taken to present the resonator with a high-impedance environment. The problem we have studied is not specific to mechanical resonators with magnetic coupling: electrostatically-driven oscillators are similarly limited by losses in the external circuit, through the electrostatic coupling capacitance [18], although the detailed dependence differs from that given here.
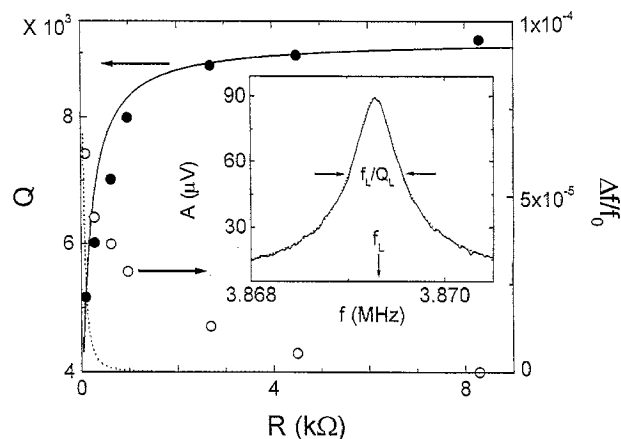

Fig. 5. Quality factor and resonance frequency measured as a function of the variable resistance. The solid dots are the measured Q values and the open dots the measured fractional frequency shift from 3.8693 MHz. The solid line is the prediction of the external circuit model for the quality factor, while the dotted line (lower left of figure) is for the frequency shift. *Inset:* Typical resonance curve (solid line), with a superposed Lorentzian fit (dotted line) to the resonance frequency $f_L = 3.86929$ MHz and quality factor $Q_L = 9310$. This curve was measured with $Q1$'s drain-source resistance set to 8.3 kΩ.

5. Summary

In conclusion, we have demonstrated that we can modulate the quality factor of a mechanical resonator by a factor of two by electrically controlling the embedding impedance presented to the resonator. Larger modulation can easily be achieved by using FETs with higher drain-source conductance. This technique can be very useful for applications that require in situ control of the quality factor, such as signal processing, where resonators are used as frequency-selective or frequency-determining elements. The result also illustrates that care must be taken to ensure that a magnetically- or electrostatically-coupled resonators are not loaded by the external drive circuit. This indicates that at very high frequencies, where obtaining large embedding impedances is problematic, attaining high quality factors will be especially challenging.

Acknowledgements

References

[1] R.E. Mihailovich, J.M. Parpia, Phys. Rev. Lett. 68 (1992) 3052.
[2] D.S. Greywall et al., Phys. Rev. Lett. 72 (1994) 2992.
[3] D.S. Greywall, B. Yurke, P.A. Busch, S. Arney, Europhys. Lett. 34 (1996) 37.
[4] B. Yurke, D.S. Greywall, A.N. Pargellis, P.A. Busch, Phys. Rev. A 51 (1995) 4211.
[5] W.C. Tang, T.C.H. Nguyen, M.W. Judy, R.T. Howe, Sensors and Actuators A21 (1990) 328.
[6] P. Cheung, R. Horowitz, R.T. Howe, IEEE Magnet 32 (1996) 122.
[7] K. Ikeda et al., Sensors and Actuators A21–A23 (1990) 1007.
[8] R.E. Mihailovich, N.C. MacDonald, Sensors and Actuators A50 (1995) 199.
[9] M. Tortonese, R.C. Barrett, C.F. Quate, Appl. Phys. Lett. 62 (1993) 834.
[10] J.D. Zook et al., Sensors and Actuators A52 (1996) 92.
[11] D.W. Burns et al., Sensors and Actuators A48 (1995) 179.
[12] A.N. Cleland, M.L. Roukes, unpublished.
[13] A.N. Cleland, M.L. Roukes, Appl. Phys. Lett. 69 (1996) 2653.
[14] W.C. Tang, T.-C.H. Nguyen, R.T. Howe, Sensors and Actuators 20 (1989) 25–32.
[15] L. Lin, C.T.-C. Nguyen, R.T. Howe, A.P. Pisano, Technical Digest, IEEE Micro Electromechanical Systems Workshop, Feb. 4–7, 1992, Travemunde, Germany, pp. 226–231.
[16] A.N. Cleland, M.L. Roukes, Nature 392 (1998) 160.
[17] R.L. Beurle, IEE Proc. 103B (1956) 182.
[18] R.E. Mihailovich, Low temperature mechanical properties of boron-doped single crystal silicon, PhD thesis, Cornell University, 1992.